Astrocytic *lactoferrin* deficiency augments MPTP-induced dopaminergic neuron loss by disturbing ER-mitochondria signaling

Shuang-Feng Xu
Northeastern University
Zhong-Qiu Pang
Northeastern University
Chen-Yang Bai
Northeastern University
Meng-Yu Jia
Northeastern University
Jun-He Cui
Northeastern University
Zhuo-Jue Wang
Northeastern University
Xiu-Ting Liang
Northeastern University
Chuang Guo (guoc@mail.neu.edu.cn)
Northeastern University https://orcid.org/0000-0003-2929-3786

Research Article

Keywords: Lactoferrin, astrocyte, Parkinson's disease, mitochondrial dysfunctions, calcium homeostasis

Posted Date: April 26th, 2022

DOI: https://doi.org/10.21203/rs.3.rs-1558216/v1

Abstract

Increased levels of lactoferrin (Lf) are present in the aged brain and in the lesions of various neurodegenerative diseases, including Parkinson's disease (PD), may contribute to the cascade of events involved in neurodevelopment and neuroprotection. However, whether Lf originates from astrocytes and functions within either the normal or pathological brain are unknown. Here, we employed mice with specific knockout of the astrocyte Lf gene (named *Lf*-cKO) to explore its specific roles in the pathological process of PD. We observed a decrease in tyrosine hydroxylase (TH)-positive cells, mitochondrial dysfunction of residual dopaminergic neurons, and motor deficits in *Lf*-cKO mice, which were significantly aggravated after 1-methyl-4-phenyl-1,2,3,6-tetrahydropyridine (MPTP) treatment. To further explore how astrocytic Lf deficiency exacerbated PD-like manifestation in MPTP-treated mice, the critical molecules involved in endoplasmic reticulum (ER)-mitochondria contacts and signaling pathways were investigated. In in vitro and in vivo models, we found an aberrant level of effects implicated in reactive oxygen species (ROS) production, apoptosis, mitochondrial morphology and functions, mitochondrial dynamics, mitochondria-associated ER membranes (MAMs), lipid metabolism, and calcium homeostasis, accompanied by signs of ER stress, which increase the fragility of dopaminergic neurons. These findings confirm the existence of astrocytic Lf and its influence on the fate of dopaminergic neurons by regulating ER-mitochondria signaling. Our findings may be a promising target for the treatment of PD.

Introduction

Parkinson's disease (PD) is a progressive neurodegenerative disease, and the main clinical manifestations include dyskinesia, bradykinesia, postural instability, gait disorder and tremor. The neuropathological core of PD is the progressive degeneration and loss of dopaminergic neurons in the substantia nigra compacta (SNpc) [1,2]. In the course of disease, PD is often accompanied by impairment of nonmotor function, such as dementia, hyposmia and gastrointestinal changes [3,4]. Although mitochondrial dysfunction and dysregulation of iron metabolism have been regarded as vital factors in the disease [5,6], the underlying mechanisms require further elucidation.

Lactoferrin (Lf), a multifunctional glycoprotein with potential clinical application value, has recently attracted extensive attention for its neuroprotective effect [7,8]. Our previous results showed that exogenous Lf treatment could ameliorate dopamine (DA) cell neurodegeneration and motor deficits in MPTP-treated mice [9]. In fact, Lf is expressed in the brains of PD patients and mouse models [10–13]. Lf receptor (LfR) is located on the surface of the vascular endothelium and DA neurons, and its expression is also increased in PD patients and mouse models [14]. Naturally, it is reasonable to hypothesize that the Lf in the brains of PD patients derives from circulating or infiltrating microglia [8]. However, the expression of Lf in astrocytes and changes in astrocytes themselves [15–17] suggest the existence of astrocytic Lf and are closely related to the pathogenesis of neurodegenerative diseases, including PD; however, whether and how Lf affects the pathogenesis and pathology of PD remains to be answered.

When exploring the neuroprotective effect of exogenous Lf on PD, it was found that Lf regulates mitochondrial function and calcium homeostasis [18–21]. Our preliminary studies found that Lf regulates lipid metabolism, such as cholesterol [22], and it has been reported that mitochondria are essential in steroid hormone synthesis, a process that begins in mitochondria [23,24]. The intracellular link between calcium and sterol involves mitochondria-associated endoplasmic reticulum (ER) membranes (MAMs) [25]. PD-related gene mutations can lead to mitochondrial rupture and reduce MAM function, increase the physical interaction between the ER and mitochondria [26,27], and promote the transfer of Ca^{2+} from the ER to mitochondria [28,29]. The change in the level of the MAM marker protein mitofusin 2 (Mfn2) indicates that the structural homeostasis of ER-mitochondria is changed in PD [25]. These findings suggest that astrocytic Lf may affect the pathological process of PD by disturbing the structure and function of MAMs. To test this hypothesis, we specifically knocked out the astrocytic *lactoferrin* gene, established a PD mouse model, and then explored specific mechanisms. The research results may provide evidence for revealing the underlying mechanism of DA neuron death in the SN, and expect to provide safe and effective targets for the prevention and treatment of PD.

Materials And Methods

Animals and treatments

Lactoferrin$^{lox/lox}$ mice were generated by introducing the loxP site between both sides of exon 3 and a neomycin selection box (Shanghai model organism). In addition, hGFAP-Cre-IRES-LacZ transgenic mice have been described [30]. In the following generation, we obtained mice with the genotype hGFAP-Cre-Lactoferrin$^{loxP/loxP}$, called "*Lf*-cKO". WT littermates were the control subjects. All male WT and *Lf*-cKO mice were randomly divided into two groups at the age of 3 months: the vehicle-treated group received 0.9% NaCl, and the MPTP-treated group received 30 mg/kg MPTP (Sigma-Aldrich, M0896). These mice were injected with MPTP or NaCl into the abdomens once a day for 5 days to produce an experimental PD model and its control.

Open field test (OFT)

The detailed method of the OFT was the same as described previously [31]. According to the experimental requirements, analysis and export of different experimental parameters.

Pole climbing test

The specific method of pole climbing test is the same as that described in previous studies [9], the time of mice passing through the upper and lower segments was recorded respectively, and then different scores were given according to the previous description [9].

Suspension test

The specific practice of suspension experiment has been shown in our previous research [9], the time of hanging on the grid was recorded, and different scores were given according to the scoring standard, so as to analyze.

Gait analysis experiment

The method of gait analysis experiment is described in previously published articles [9]. Step length, step width, average variation of distance between two adjacent left or right footprints, gait variation rate and other indicators can reflect the ataxia movement of experimental rats.

Immunohistochemistry and immunofluorescence

The immunohistochemistry and immunofluorescence processes were described specifically in our previous experiment [6,7]. For immunohistochemistry, the slices were incubated with rabbit anti-tyrosine hydroxylase (TH, 1:800; Millipore), rat anti-dopamine transporter (DAT, 1:800; Millipore) and mouse anti-α-synuclein (1:600; Thermo Fisher Scientific). For immunofluorescence staining, the mice brain slices were respectively co-incubated with rabbit anti-TH (1:600; Millipore) and mouse anti-parkin RBR E3 ubiquitin protein ligase (PARK2/Parkin, 1:200; Proteintech); mouse anti-Tom20 (1:400; Santa Cruz) and rabbit anti-KDEL-ER (1:400; Thermo Fisher Scientific); rabbit anti-TH (1:600; Millipore) and goat anti-steroidogenic acute regulatory protein (StAR, 1:200; Santa Cruz). Primary astrocytes were co-incubated with mouse anti-glial fibrillary acidic protein (GFAP, 1:400; Thermo Fisher Scientific) and goat anti-StAR (1:200; Santa Cruz). MN9D cells (mouse midbrain dopaminergic neuron cell line) were co-incubated with mouse anti-Tom20 (1:200; Santa Cruz) and rabbit anti-TH (1:600; Millipore), rabbit anti-TH (1:600; Millipore) and goat anti-StAR (1:200; Santa Cruz).

Improved iron staining

On the basis of Prussian blue staining, an improved iron staining method was used to detect the iron content, the detailed method was the same as described previously [32,33].

Electron Microscopy analysis

For electron microscopy, samples were dissected and postfixed overnight in the fixative buffer (2% glutaraldehyde/2% paraformaldehyde in 0.1 M cacodylate buffer). Tissues were processed using a standard procedure before imaging.

Western blot analyses

Extraction all the mice striatum and SN and striatum tissues or cells protein, and the procedure and method of western blots were the same as described previously [6]. The primary antibodies required for this experiment were shown as Table 1.

Cells culture and treatment

Tail biopsies (P0) were used for genotyping. Astrocytes were isolated from the cerebral cortex of WT and *Lf*-cKO mice (P0; n = 5 per genotype), and the specific extraction process was carried out according to a previously described method [34,35]. For coculture, medium was harvested from WT and *Lf*-cKO astrocytes after 24 h to culture MN9D cells. For cell treatment, cells were starved in FBS-free medium for 12 h before being treated with N-methyl-4-phenylpyridinium (MPP^+, 1 mM; D048; Sigma-Aldrich) treatment for 24 h.

Quantitative Real-time PCR (qPCR)

Total RNA was extracted from tissues or primary astrocytes using TRIzol reagent (Vazyme; R410-1). mRNA (1000 ng) was reverse transcribed into cDNA using MonScript^{TM} RTIII All-in-One Mix (Monad; RN05003S). The primer sequences and the related SYBR Green probes are shown: GAPDH (TGCAGTGGCAAAGTGGAGAT and TTTGCCGTGAGTGGAGTCTA), mitochondrial trifunctional protein (MTP, ACCTACCAGGCCCAGCAAGA and ACACCTGCCACTTGCTTCCC), StAR (GCAGGAGAACGGGGACGAAG and CTGCCAGCACACAGGTGGAA).

Detection of malondialdehyde (MDA) and reactive oxygen species (ROS)

In this experiment, the MDA test kit (A003-2, TBA method, Nanjing Jiancheng Bioengineering Institute) was used for detection, calculation and analysis according to the manufacturer's protocol. ROS production was measured using 2', 7'-dichlorofluorescein diacetates (DCFH-DA) according to the manufacturer's protocol (E004, Jiancheng Biology, Nanjing, China). The detailed method was the same as described previously [31].

Determination of intracellular calcium concentration

The concentration of intracellular calcium was performed and analyzed by flow cytometry (BD LSRFortessa) as previously described [36,37].

Glycolysis experiment

The specific experimental method of glycolysis experiment was carried out with reference to the published papers [38]. The measurement, output and analysis of experimental data were performed by Agilent Seahorse cell energy metabolism analyzer (XFe96).

Statistics

All experimental data are expressed as the mean ± standard error of the mean (SEM). All date were obtained from more than three independent repeated experiments and were analyzed using GraphPad Prism 7. When comparing the differences between the data groups, one way ANOVA test was used for the data conforming to the normal distribution followed by Tukey's multiple comparison groups; for the data that did not conform to the normal distribution, the Kruskal Wallis test was used, followed by Dunn's

multiple comparison test. The difference of significance is expressed by *p* value. A *p*-value less than 0.01, is very significant, and a *p*-value less than 0.05 is statistically significant.

Results

3.1 Astrocyte-specific loss of *Lf* increases MPTP-induced behavioral and emotional disorder

Our parallel experiment confirmed the existence of astrocyte Lf and its significance for early neuronal development (Data not presented). Here, the body weight of *Lf*-cKO mice was lower than that of the litter control mice and wild control mice at 3 months of age (Fig 1A, B). To determine whether astrocytic Lf deficiency induces PD-like symptoms in mice, we carried out several behavioral tests. The results demonstrate that the motor activity and emotional responses of *Lf*-cKO mice were significantly reduced compared with the control group; after MPTP treatment, the decrease was more significant in the OFT (Fig 1C, D). The results showed that the motor ability of *Lf*-cKO mice was significantly reduced compared with that of the control group in the climbing pole and the hanging experiments, while MPTP treatment enhanced this effect in the hanging experiment (Fig 1E, F). As seen from the gait analysis experiment (Fig 1G-J), the gait variability, step width variability and other indicators in *Lf*-cKO mice were increased compared with those of the control group, indicating ataxia and weakness in mice, and this effect was more significant after MPTP treatment. The results of several behavioral tests suggest that astrocytic Lf deficiency leads to PD-like manifestations in mice, which are aggravated by MPTP administration.

3.2 DA neuron degeneration is more pronounced in MPTP-treated *Lf*-cKO mice

To investigate the reason for behavioral deficits in *Lf*-cKO mice, we used immunohistochemistry to detect nigrostriatal lesions. As shown in Fig 2A, TH- and DAT-positive staining was significantly decreased in *Lf*-cKO mice, and the effect was more significant after MPTP administration. The protein level test results showed that the changes in TH and DAT were consistent with the immunohistochemistry results (Fig 2B-D). Moreover, both immunostaining and Western blotting showed that the expression of α-synuclein was significantly increased in *Lf*-cKO mice, and the increasing trend was more dramatic after MPTP treatment (Fig 2A, B, E) than in the control group. These results suggest that astrocytic Lf deficiency can lead to the loss of dopaminergic neurons and an increase in α-synuclein, which was more sensitive after MPTP treatment.

Given the loss of dopaminergic neurons, we analyzed apoptosis-related proteins by Western blotting. Fig 2F-H shows that the protein expression of cleaved-caspase3 in *Lf*-cKO mice was significantly increased and the ratio of Bcl-2/Bax was significantly decreased, compared with that in the control group. After MPTP treatment, these changes in cleaved-caspase3 and Bcl-2/Bax values were further exacerbated in *Lf*-cKO mice. In special cases, such as ER stress, autophagy-related proteins may promote apoptosis [39]. As shown in Fig 2F, I, the level of autophagy protein 5 (ATG5) was increased after *Lf* knockout or MPTP treatment, but the increase was not significant. These results indicated that the antiapoptotic ability of DA cells was weakened after astrocytic Lf deficiency and that apoptosis was more pronounced after MPTP treatment.

3.3 Astrocytic Lf deficiency induces iron metabolism disorder and aggravates oxidative stress in MPTP-treated mice

Lf is a member of the transferrin family, and its well-known function is to regulate iron homeostasis [8]. To observe whether *Lf* knockout in astrocytes affects iron homeostasis in the SN of mice, we carried out Perl's DAB iron staining. As shown in Fig 3A, there was no increase in iron accumulation in the neuronal cytoplasm in the SN of the *Lf*-cKO mice than in the controls, and after MPTP treatment, there were substantially more iron-positive cells than in the other mice, which suggests that astrocytic Lf deficiency enhances MPTP-induced iron accumulation. Next, we quantitatively analyzed iron-related transporters. As shown in Fig 3B-E, the expression level of ferroportin (Fpn) was significantly decreased in *Lf*-cKO mice compared with the controls, and the decrease was more significant after MPTP treatment. Moreover, MPTP-induced transferrin receptor (TfR) upregulation was further exacerbated in *Lf*-cKO mice. However, the expression of divalent metal transporter 1 (DMT1) was not significantly different. These findings indicate that the loss of Lf in astrocytes may not directly lead to iron homeostasis disorder, but can cause the imbalance of iron homeostasis, and even aggravate the MPTP-induced iron accumulation in SN.

Oxidative stress plays critical roles in PD pathogenesis [40], and Lf can inhibit oxidative stress [41]. We first detected the expression of glutathione peroxidase 4 (GPX4), superoxide dismutase (SOD1) and cystine/glutamate exchange transporter (xCT). The level of antioxidant enzymes significantly decreased in *Lf*-cKO mice, and MPTP administration induced further downregulation of xCT expression (Fig 3F-I). Consistently, ROS content was significantly increased in *Lf*-cKO mice compared with the control; the change was more significant after MPTP treatment (Fig 3J). In addition, MPTP treatment clearly increased the level of MDA; however, MDA content in *Lf*-cKO mouse brain tissues was not significantly increased compared with controls (Fig 3K). These results indicated that the specific knockout of the *Lf* gene in astrocytes caused oxidative stress and lipid peroxidation by inhibiting the activity of antioxidant enzymes in the SN of the mouse brain.

3.4 Astrocytic Lf deficiency leads to mitochondrial dysfunction of dopaminergic neurons and is aggravated after MPTP treatment

To understand the mechanisms by which dopaminergic neurons in *Lf*-cKO mice are more vulnerable to neurotoxicity, we used an immunofluorescence double labeling technique (Fig 4A) to label TH and PARK2/Parkin. The fluorescence results showed decreased colocalization of PARK2/Parkin and TH in *Lf*-cKO mice. Although PARK2/Parkin expression did not decrease, except in TH-positive neurons, these results suggest that the mitochondrial function of DA neurons was impaired. As expected, after MPTP administration, the change in PARK2/Parkin expression in residual neurons was more significant with the loss of DA cells in *Lf*-cKO mice. Next, we detected several proteins related to mitochondrial function, such as Cytochromes c (CytC), Cytochrome C Oxidase Subunit 4 (COX4), PTEN-induced kinase 1 (PINK1), PARK2/Parkin and heat shock protein 60 (HSP60). As shown in Fig 4B-G, compared with the control group, the expression levels of CytC and PARK2/Parkin in the brains of *Lf*-cKO mice were increased, while the expression level of HSP60 was significantly decreased. After MPTP treatment, the upregulation of

CytC and downregulation of HSP60 were further exacerbated in the brains of *Lf*-cKO mice, while the alteration of PARK2/Parkin was significantly reversed. Moreover, MPTP treatment led to decreased COX4 expression in the brains of *Lf*-cKO mice, but PINK1 expression was not significantly changed by *Lf* knockout and subsequent MPTP treatment compared with control mice. In addition, as shown in Fig 4H-J, compared with control mice, phosphorylated-Dynamin related peptide 1 Ser637 (p-Drp1^{S637}) expression was clearly decreased in the SN of *Lf*-cKO mice; however, the upregulation of p-Drp1^{S637} expression induced by MPTP treatment was not significantly different between *Lf*-cKO mice and control mice. These data suggested that astrocytic Lf deficiency leads to mitochondrial dysfunction and fragmentation, and these changes are more sensitive after MPTP administration.

3.5 Astrocytic Lf deficiency induces mitochondrial dysfunction and neuronal apoptosis in vitro

To further evaluate the mechanisms that underlie the specific knockout of astrocyte *Lf* on mitochondrial dysfunction, we performed immunofluorescence of Tom20 (a mitochondrial marker) on DA neurons. As shown in Fig 5A, after MN9D cells were cultured with astrocyte culture medium extracted from control or *Lf*-cKO newborn mice, the immunoreactive intensity of TH and Tom20 in the latter group was weaker than that in the former group, and this change was more significant after treatment with MPP^+. Western blot results showed that the expression levels of TH, Mfn2 and PARK2/Parkin in MN9D cells cocultured with Lf gene knockout primary astrocytes were significantly lower than those in MN9D cells cocultured with WT primary astrocytes (Fig 5B-G). After MPP^+ treatment, the difference was extremely significant. Moreover, the change trend of the Bcl-2/Bax ratio and cleaved-caspase3 induced by several treatment factors suggests that astrocytic Lf deficiency can cause apoptosis of dopaminergic neurons. In addition, we also examined the cellular bioenergy of MN9D cells after different treatments (Fig 5H). We observed that the lack of astrocyte-derived Lf resulted in decreased glycolysis levels, glycolysis maximum values and glycolysis reserve values, and the changes in each index were more obvious after MPP^+ treatment in MN9D cells. The above results further revealed that astrocyte-derived Lf plays an important role in the regulation of mitochondrial function and even the survival of dopaminergic neurons.

3.6 Astrocyte-derived Lf regulates calcium homeostasis in dopaminergic neurons

In this project, we aimed to identify the specific mechanism underlying the changes in mitochondrial dysfunctions. PD-associated mitochondrial dysfunction may result from multiple factors, and disturbance of intracellular calcium homeostasis is one of the common factors [42]. We used flow cytometry to detect the calcium concentration in MN9D cells in each group after coculture and drug administration. According to Fig 6A, compared with the control group, the calcium concentration in MN9D cells after MPP^+ treatment increased by 12.2%, and the calcium concentration of MN9D cells cocultured with WT primary astrocytes increased by 17.6% after MPP^+ treatment. Interestingly, the intracellular calcium concentration of MN9D cells cocultured with *Lf* knockout primary astrocytes decreased by 27%, while the calcium concentration greatly increased by 25.9% after MPP^+ treatment. The results indicated

that the lack of astrocyte-derived Lf may disturb calcium homeostasis in MN9D cells, and significantly increase the MPP^+-induced upregulation of intracellular calcium levels.

Elevated intracellular Ca^{2+} levels activate a variety of Ca^{2+}-dependent proteins and kinases. According to Fig 6B-F, Ca^{2+}/calmodulin-dependent protein kinase α (CAMKIIα) levels were significantly increased in *Lf*-cKO mice compared with controls. Moreover, the increase in CAMKIIα levels was significantly decreased after MPTP treatment, as seen in control mice. However, there were no significant differences in calreticulin and calmodulin levels in the nigrostriatal region between *Lf*-cKO mice and control mice, but the increase in calreticulin and calmodulin levels in the brains of *Lf*-cKO mice was more obvious after MPTP treatment. Notably, we detected that N-methyl-D-aspartate receptor subunit 2B (NMDAR2B) was less abundant in the SN of *Lf*-cKO mice than in control mice, but its expression was dramatically upregulated after MPTP treatment. These results suggest that astrocyte-derived Lf plays an important role in regulating calcium homeostasis.

3.7 Astrocyte-derived Lf deficiency-induced intracellular calcium dyshomeostasis involves the ER

We further determined the mechanism and effect of astrocyte-derived Lf deficiency-induced calcium disorders in dopaminergic neurons. The results (Fig 7A-C) showed that after MPP^+ treatment, the level of CAMKIIα was markedly declined in the group that was cocultured with *Lf*-cKO primary astrocytes, and the reduction was no longer augmented by MPP^+ treatment. Although this result is inconsistent with previous in vivo results, it can be suggested that astrocyte-derived Lf deficiency may disturb Ca^{2+} homeostasis in dopaminergic neurons by controlling CAMKIIα.

The ER stores many calcium ions, and the influx of Ca^{2+} will cause mitochondrial dysfunction and disruption [43]. Naturally, we then tested whether ER stress occurred in the brains of mice in each group. As exhibited in Fig 7D-F, the p-eukaryotic translation initiation factor 2α (p-EIF2α) level in *Lf*-cKO mice was significantly increased compared with that in the controls, and the level was obviously reduced after MPTP treatment. Moreover, the level of p-EIF2α in the MPTP-treated *Lf*-cKO mice was also higher than that in the MPTP-treated control mice, suggesting the occurrence of ER stress. In addition, as shown in Fig 7G, immunofluorescence results using coimmunoprecipitation of KDEL-ER (ER marker, red) and Tom20 (mitochondria marker, green) indicated higher immunoreactivity intensity of KDEL-ER in the DA neurons of *Lf*-cKO mice than that in control mice, accompanied by an increased immunoreactivity of Tom20. However, treatment with MPTP significantly decreased KDEL-ER and Tom20 immunoreactive intensity in *Lf*-cKO mice compared with the controls. These results suggest that loss of astrocyte-derived Lf may play a key role in the disruption of ER structure, distribution, and function in DA neurons and aggravate MPTP-induced cytotoxicity.

3.8 Astrocyte-derived Lf deficiency prevents mitochondrial lipid transport by affecting MAMs

MAMs are scaffolds between mitochondria and the ER that regulate ER function, mitochondrial physiology and metabolite exchange and are involved in calcium homeostasis and lipid metabolism [44].

As shown by the electron microscopy results (Fig 8A), compared with the control group, the mitochondria in neurons of *Lf*-cKO mice had shorter and rounder shapes, poor continuity of the mitochondrial network and closer connections with the ER. Moreover, we found that MPTP downregulated the level of Mfn2, but the level of Mfn2 was relatively stable in *Lf*-cKO mice before and after MPTP treatment compared with the control mice (Fig 8B, C), suggesting ER-mitochondria tethering damage.

To further clarify the mechanism of Lf acting on mitochondrial disruption, we detected the mRNA levels of StAR and MTP using qPCR. The levels of StAR and MTP mRNA were observably decreased in *Lf*-cKO mice compared with controls, and the difference in decline was more significant in MPTP-treated mice (Fig 8D, E). Moreover, the expression of StAR was visualized using immunofluorescence in vivo and in vitro (Fig 8F-H). Immunostaining showed that StAR expression was mostly restricted to TH-positive cells, and its expression was decreased in mice with loss of astrocyte derived Lf. As expected, StAR expression was further reduced, which was accompanied by a reduction in TH expression in the MPTP treatment group compared to the controls, indicating that the induced reductions in StAR expression are highly correlated with the loss of dopaminergic neurons in *Lf*-cKO mice and PD mouse models. Congruously, astrocytic Lf deficiency slightly or significantly reduced StAR expression in primary astrocytes or MN9D cells, respectively, whereas the MPTP-induced reduction was significant in various cells. These results indicate that after astrocytic *Lf* knockout, there was a decrease in the transport of steroids and lipids to mitochondria, resulting in the mitochondrial dysfunction of dopaminergic neurons, and these changes are exacerbated after administration of MPTP.

Discussion

Our previous studies have shown that endogenous Lf supplementation effectively ameliorates the neuropathology of neurodegenerative disease and behavioral disorders [7,9]. Notably, growing evidence supports that nerve cells, including microglia, can also synthesize Lf [11], but whether Lf can be produced by astrocytes and how its functions need to be clarified. In this study, we verified that astrocytic Lf deficiency aggravated MPTP-induced loss of dopaminergic neurons and motor deficits in mice by regulating ER-mitochondria signaling (Fig. 9).

Because the neurons in the SN of PD patients can highly express Lf and LfR [12,14], it is naturally speculated that Lf is derived from the extracellular space [45]. Later experiments confirmed that activated microglia in a PD animal model can synthesize Lf [11]. To date, the source of Lf in the brain has rarely been explored. However, after reviewing the relevant literature, we noticed that Lf played an important role in the early development of the brain and was positively correlated with BDNF, which is mainly secreted by astrocytes [45], and Lf was detected in astrocytes of the elderly brains in Alzheimer's disease (AD) and normal human brains [17]. Therefore, we speculated that astrocytes could synthesize Lf, but this function was more obvious in some stages of brain development or pathological conditions. Here, we bred mice with specific knockout of astrocytic Lf for systematic study. Although we observed increased Lf expression in microglia and capillaries of *Lf*-cKO mice compared with control mice (Fig S1-3), under MPTP induction, *Lf*-cKO mice showed more severe motor impairment and DA neuron loss. In addition, *Lf*-

cKO mice had PD-like pathology and symptoms. These data not only confirmed that astrocyte-derived Lf was involved in the regulation of the function and survival of dopaminergic neurons but also suggest that circulating Lf and microglia-secreted Lf are not enough to protect dopamine neurons from the pathogenesis of PD.

Our recent study demonstrated that iron deposition in the SN-striatum system is an early event in PD [46]. Since Lf is a member of the transferrin family, we first examined whether the deletion of astrocyte Lf perturbs iron metabolism in the SN of mice. According to the iron staining results, there was no significant increase in iron deposition in the SN of *Lf*-cKO mice; however, the MPTP-induced iron accumulation in *Lf*-cKO mice was larger than that in control mice. Accordingly, increased intracellular iron input protein TFR and decreased extracellular output protein Fpn in MPTP-treated *Lf*-cKO mice can explain the changes of iron levels in PD lesions. Based on the changes in iron and several iron transport-related proteins, knocking out the *Lf* in astrocytes has an effect on iron metabolism in the nigrostriatal region, but it is not the main cause of DA neuron apoptosis.

The antioxidant properties of Lf have been highlighted in MPTP-induced PD models [18,9]. Here, we demonstrated that the level of MDA (a marker of lipid peroxidation) in *Lf*-cKO mice did not show any significant differences compared to controls; however, ROS production was markedly increased and the xCT and mitochondria containing two of antioxidant enzymes copper/zinc SOD1 and GPX4 were clearly decreased in *Lf*-cKO mice, suggesting loss of astrocytic Lf induces neuronal mitochondria-dependent apoptosis following cellular redox activity. Indeed, a region-specific reduction in the glutathione/GPX system and SOD1 protein expression are characteristics of preclinical PD, prior to neuronal loss and oxidative stress in the aging substantia nigra and the etiology of PD [40]. Supporting a role for astrocytic Lf in antioxidant activity rather than controlling ROS generation, the levels of MDA, ROS, α-synuclein, iron accumulation, and dopaminergic neuronal apoptosis in *Lf*-cKO mice were dramatically aggravated following MPTP administration, whereas the expression of SOD1 and GPX4 was not significantly affected. Another proposed antioxidative mechanism of Lf is as a receptor of the electron transport chain and stimulation of glycolysis [47]. Importantly, regardless of the mechanism, the above data suggest that the loss of dopaminergic neurons in the brains of *Lf*-cKO mice may be related to mitochondrial dysfunction.

In fact, it has been proposed that the neuroprotective efficiency of Lf on dopaminergic neurons is equivalent to glial cell line-derived neurotrophic factor, and mitochondria may be its downstream target [48]. Although the function of Lf in astrocytes cannot be fully clarified, the current findings support the hypothesis that Lf may affect the survival of dopaminergic neurons by directly or indirectly regulating mitochondrial function.

To better understand the role of astrocytic Lf deficiency in mitochondrial dysfunction, we sought to identify the structure and function of mitochondria in dopaminergic neurons of *Lf*-cKO mice. The following important findings further demonstrate a role of astrocytic Lf deficiency in mitochondrial dysfunction in dopaminergic neurons of *Lf*-cKO mice: 1) CytC, a pro-apoptotic protein which plays an

important role in mitochondrial electron transport chain (ETC) [49,50], was markedly upregulated; 2): increased levels of PARK2/Parkin (a key mitophagy protein) colocalized with TH-positive neurons in *Lf*-cKO mice and were correlated with autosomal recessive early onset PD [51]; 3): decreased levels of mitochondrial stress protein HSP60, which help provoke mitochondrial and cellular dyshomeostasis[52]; 4): although the expression of Drp1, a key regulator of mitochondrial dynamics, was slightly upregulated, the phosphorylation of Drp1 at S637 site was significantly inhibited, suggesting that Drp1 activity and mitochondrial dynamics are impaired in *Lf*-cKO mice[53]; 5): decreased intracellular calcium concentration in MN9D cells cocultured with Lf knockout primary astrocytes and decreased NMDAR2B protein levels and overexpression of CAMKIIα protein in *Lf*-cKO mice demonstrated that Ca^{2+} buffering was impaired [54]. Of course, the low cytosolic Ca^{2+} buffering in the cocultured dopaminergic neurons may be mainly related to large amounts of Ca^{2+} intake from the cytosol by mitochondria, which can evoke mitochondrial dynamics and fission[55,56]; 6): more importantly, in the neurons of *Lf*-cKO mice, we observed round and broken mitochondria by electron microscopy. Although some of the mitochondrial changes we observed may be compensatory, more negative evidence (such as decreased ROS clearance, ETC dysfunction, defective mitophagy, Ca^{2+} imbalance, variations in mitochondrial dynamics and morphology) supports that the deletion of Lf in astrocytes contributes to PD-associated mitochondrial dysfunction and neuronal apoptosis. Unsurprisingly, after *Lf*-cKO mice were treated with MPTP, the variations of various mitochondrial dysfunction and apoptosis indices became consistent and intensified. Consistently, we verified in vitro the changes in various mitochondrial dysfunction and apoptosis indexes caused by the lack of astrocyte-derived Lf and analyzed the ECAR value to demonstrate a decrease in glycolysis level, maximum glycolysis and glycolysis reserve; however, these data cannot exclude those other indirect unrelated pathways influencing the mitochondrial function of dopaminergic neurons.

Unexpectedly, we cocultured primary astrocytes of *Lf*-cKO mice with MN9D cells and found that Ca^{2+} concentrations in neuronal cytoplasm decreased significantly. It is speculated that imported Ca^{2+} may be stored in mitochondria and the ER [40]. At this time, the increased in p-EIF2α levels indicates that ER stress occurs in the brains of *Lf*-cKO mice, which also supports this hypothesis. After MPP^+ treatment, the sharp increase in intracellular Ca^{2+} could mainly come from extracellular influx because the calcium channel proteins NMDAR2B and calmodulin were upregulated, which can trigger an increased in neuronal vulnerability [57]. Nevertheless, the increased calcium binding proteins of ER calreticulin and the decreased p-EIF2α indicated that Ca^{2+} in the ER seemed to decrease, and α-synuclein overexpression may stimulate the release of Ca^{2+} in the ER or transfer to mitochondria after MPP^+ treatment [58].

In fact, mitochondria have been shown to share structural and functional communication with the ER to maintain intracellular calcium homeostasis and lipid metabolism [59]. Mitochondria-associated ER membrane-specific microdomains are mediated by tethering proteins, and altered ER-mitochondria tethering and perturbed ER-mitochondria communication may contribute to neurodegeneration in PD [25]. Mfn2, a MAM resident protein, is considered to be a key ER-mitochondrial tether [25]. Our study determined that the Mfn2 protein decreased slightly in *Lf*-cKO mice, which was exacerbated by MPTP

treatment, indicating that the knockout of *Lf* in astrocytes makes contact between mitochondria and the ER closer in dopaminergic neurons [60]. Accordingly, electron microscopy and confocal microscopy images revealed that the ER-mitochondria distance was reduced in *Lf*-cKO mice compared with control mice. In addition, MAMs have unique lipid and protein components for effective interaction between the ER and mitochondria [61–63]. StAR is also a MAM protein and is involved in the continuous influx of cholesterol into mitochondria, thereby initiating mitochondrial steroidogenesis [64]. In this study, we detected decreased StAR and MTP (an enzymatic complex located in the inner mitochondrial membrane and responsible for β-oxidation of long-chain fatty acids) [65] mRNA levels in *Lf*-cKO mice. Moreover, astrocytic Lf deficiency led to a reduction in StAR protein in primary astrocytes or dopaminergic neurons in vivo and in vitro, and the difference was more significant after MPTP or administration of metabolite MPP^+. In other words, astrocyte-derived Lf deficiency leads to impaired cholesterol transfer and mitochondrial fusion/fission cycles, which subsequently impacts the structure and function of neuronal MAMs [66,67].

In conclusion, our current study confirmed that the lack of astrocyte-derived Lf can worsen MPTP-induced PD-like neuropathology and symptoms by increasing the fragility of dopaminergic neurons. Admittedly, insight into its underlying mechanisms requires greater study, but findings emerged showing that after the deletion of the Lf gene in astrocytes, the intracellular homeostasis of dopaminergic neurons is unbalanced and that the factors causing PD accumulate, such as overproduction of ROS, alteration of calcium homeostasis, and dysfunctional mitochondria (especially MAM dysfunction) [56,68,25,53,40]. Of course, further research is needed to investigate exactly what kind of compensation mechanism is activated by Lf in astrocytes to maintain the function and state of neurons.

Abbreviations

AD, Alzheimer's disease; ATG5, autophagy protein 5; BDNF, brain-derived neurotrophic factor; CAMKIIα, Ca^{2+}/calmodulin-dependent protein kinase α; CytC, Cytochromes c; COX4, Cytochrome C Oxidase Subunit 4; DA, dopamine; DAT, dopamine transporter; DMT1, divalent metal transporter 1; ER, endoplasmic reticulum; ETC, electron transport chain; Fpn; ferroportin; GPX4, glutathione peroxidase 4; HSP60, heat shock protein 60; Lf, lactoferrin; LfR, lactoferrin receptor MAMs, mitochondria-associated ER membranes; GFAP, glial fibrillary acidic protein; MDA, malondialdehyde; Mfn2, mitofusin 2; MPTP, 1-methyl-4-phenyl-1,2,3,6-tetrahydropyridine; MTP, mitochondrial trifunctional protein; NMDAR2B, N-methyl-D-aspartate receptor subunit 2B; OFT, Open field test; PD, Parkinson's disease; p-Drp1^{S637}, phosphorylated-Dynamin related peptide 1 Ser637; p-EIF2α, p-eukaryotic translation initiation factor 2α; PARK2/Parkin, parkin RBR E3 ubiquitin protein ligase; PINK1, PTEN-induced kinase 1; ROS, reactive oxygen species; SNpc, substantia nigra compacta; SOD, superoxide dismutase; StAR, steroidogenic acute regulatory protein; TH, tyrosine hydroxylase; TFR, transferrin receptor; xCT, cystine/glutamate exchange transporter

Declarations

Acknowledgments

Not applicable.

Funding

The study was supported by the Natural Science Foundation of China (No. 31970967).

Conflict of Interest

The authors declare no competing interests.

Author contributions

Shuang-Feng Xu performed most of the experiments and analyzed the data; Zhong-Qiu Pang contributed to cell experiments, generated and validated the mouse model; Chen-Yang Bai, Meng-Yu Jia, Jun-He Cui, Zhuo-Jue Wang, and Xiu-Ting Liang contributed to generated and validated the mouse model; Chuang Guo, designed and wrote manuscript. All authors have read and approved the final manuscript.

Availability of data and materials

Data supporting the conclusions of this article are presented in this manuscript.

Ethics approval and consent to participate

All experimental procedures involved were performed according to protocols approved by the Laboratory Animal Ethical Committee of Northeastern University.

Consent for publication

Consent form submitted.

References

1. Mullin S, Schapira AH (2015) Pathogenic mechanisms of neurodegeneration in Parkinson disease. Neurol Clin 33 (1):1-17. http://dx.doi.org/10.1016/j.ncl.2014.09.010
2. Dauer W, Przedborski S (2003) Parkinson's disease: mechanisms and models. Neuron 39 (6):889-909. http://dx.doi.org/10.1016/s0896-6273(03)00568-3
3. Chaudhuri KR, Martinez-Martin P (2008) Quantitation of non-motor symptoms in Parkinson's disease. Eur J Neurol 15 Suppl 2:2-7. http://dx.doi.org/10.1111/j.1468-1331.2008.02212.x
4. Raza C, Anjum R, Shakeel NUA (2019) Parkinson's disease: Mechanisms, translational models and management strategies. Life Sci 226:77-90. http://dx.doi.org/10.1016/j.lfs.2019.03.057
5. Cheng A, Jia W, Kawahata I, Fukunaga K (2021) Impact of Fatty Acid-Binding Proteins in alpha-Synuclein-Induced Mitochondrial Injury in Synucleinopathy. Biomedicines 9 (5). http://dx.doi.org/10.3390/biomedicines9050560

6. Guo C, Hao LJ, Yang ZH, Chai R, Zhang S, Gu Y, Gao HL, Zhong ML, Wang T, Li JY, Wang ZY (2016) Deferoxamine-mediated up-regulation of HIF-1alpha prevents dopaminergic neuronal death via the activation of MAPK family proteins in MPTP-treated mice. Exp Neurol 280:13-23. http://dx.doi.org/10.1016/j.expneurol.2016.03.016
7. Guo C, Yang ZH, Zhang S, Chai R, Xue H, Zhang YH, Li JY, Wang ZY (2017) Intranasal Lactoferrin Enhances alpha-Secretase-Dependent Amyloid Precursor Protein Processing via the ERK1/2-CREB and HIF-1alpha Pathways in an Alzheimer's Disease Mouse Model. Neuropsychopharmacology 42 (13):2504-2515. http://dx.doi.org/10.1038/npp.2017.8
8. Li YQ, Guo C (2021) A Review on Lactoferrin and Central Nervous System Diseases. Cells 10 (7). http://dx.doi.org/10.3390/cells10071810
9. Xu SF, Zhang YH, Wang S, Pang ZQ, Fan YG, Li JY, Wang ZY, Guo C (2019) Lactoferrin ameliorates dopaminergic neurodegeneration and motor deficits in MPTP-treated mice. Redox Biol 21:101090. http://dx.doi.org/10.1016/j.redox.2018.101090
10. Grau AJ, Willig V, Fogel W, Werle E (2001) Assessment of plasma lactoferrin in Parkinson's disease. Mov Disord 16 (1):131-134. http://dx.doi.org/10.1002/1531-8257(200101)16:1<131::aid-mds1008>3.0.co;2-o
11. Fillebeen C, Ruchoux MM, Mitchell V, Vincent S, Benaissa M, Pierce A (2001) Lactoferrin is synthesized by activated microglia in the human substantia nigra and its synthesis by the human microglial CHME cell line is upregulated by tumor necrosis factor alpha or 1-methyl-4-phenylpyridinium treatment. Brain Res Mol Brain Res 96 (1-2):103-113. http://dx.doi.org/10.1016/s0169-328x(01)00216-9
12. Leveugle B, Faucheux BA, Bouras C, Nillesse N, Spik G, Hirsch EC, Agid Y, Hof PR (1996) Cellular distribution of the iron-binding protein lactotransferrin in the mesencephalon of Parkinson's disease cases. Acta Neuropathol 91 (6):566-572. http://dx.doi.org/10.1007/s004010050468
13. Fillebeen C, Mitchell V, Dexter D, Benaissa M, Beauvillain J, Spik G, Pierce A (1999) Lactoferrin is synthesized by mouse brain tissue and its expression is enhanced after MPTP treatment. Brain Res Mol Brain Res 72 (2):183-194. http://dx.doi.org/10.1016/s0169-328x(99)00221-1
14. Faucheux BA, Nillesse N, Damier P, Spik G, Mouatt-Prigent A, Pierce A, Leveugle B, Kubis N, Hauw JJ, Agid Y, et al. (1995) Expression of lactoferrin receptors is increased in the mesencephalon of patients with Parkinson disease. Proc Natl Acad Sci U S A 92 (21):9603-9607. http://dx.doi.org/10.1073/pnas.92.21.9603
15. Wang L, Sato H, Zhao S, Tooyama I (2010) Deposition of lactoferrin in fibrillar-type senile plaques in the brains of transgenic mouse models of Alzheimer's disease. Neurosci Lett 481 (3):164-167. http://dx.doi.org/10.1016/j.neulet.2010.06.079
16. Tuccari G, Giuffre G, Crisafulli C, Barresi G (1999) Immunohistochemical detection of lactoferrin in human astrocytomas and multiforme glioblastomas. Eur J Histochem 43 (4):317-322.
17. Kawamata T, Tooyama I, Yamada T, Walker DG, McGeer PL (1993) Lactotransferrin immunocytochemistry in Alzheimer and normal human brain. Am J Pathol 142 (5):1574-1585.

18. Wang J, Bi M, Liu H, Song N, Xie J (2015) The protective effect of lactoferrin on ventral mesencephalon neurons against MPP + is not connected with its iron binding ability. Sci Rep 5:10729. http://dx.doi.org/10.1038/srep10729
19. Liu H, Wu H, Zhu N, Xu Z, Wang Y, Qu Y, Wang J (2020) Lactoferrin protects against iron dysregulation, oxidative stress, and apoptosis in 1-methyl-4-phenyl-1,2,3,6-tetrahydropyridine (MPTP)-induced Parkinson's disease in mice. J Neurochem 152 (3):397-415. http://dx.doi.org/10.1111/jnc.14857
20. Gifford JL, Ishida H, Vogel HJ (2012) Structural characterization of the interaction of human lactoferrin with calmodulin. PLoS One 7 (12):e51026. http://dx.doi.org/10.1371/journal.pone.0051026
21. Grigorieva DV, Gorudko IV, Shamova EV, Terekhova MS, Maliushkova EV, Semak IV, Cherenkevich SN, Sokolov AV, Timoshenko AV (2019) Effects of recombinant human lactoferrin on calcium signaling and functional responses of human neutrophils. Arch Biochem Biophys 675:108122. http://dx.doi.org/10.1016/j.abb.2019.108122
22. Guo C, Xue H, Guo T, Zhang W, Xuan WQ, Ren YT, Wang D, Chen YH, Meng YH, Gao HL, Zhao P (2020) Recombinant human lactoferrin attenuates the progression of hepatosteatosis and hepatocellular death by regulating iron and lipid homeostasis in ob/ob mice. Food Funct 11 (8):7183-7196. http://dx.doi.org/10.1039/d0fo00910e
23. Nunnari J, Suomalainen A (2012) Mitochondria: in sickness and in health. Cell 148 (6):1145-1159. http://dx.doi.org/10.1016/j.cell.2012.02.035
24. Miller WL (2013) Steroid hormone synthesis in mitochondria. Mol Cell Endocrinol 379 (1-2):62-73. http://dx.doi.org/10.1016/j.mce.2013.04.014
25. Veeresh P, Kaur H, Sarmah D, Mounica L, Verma G, Kotian V, Kesharwani R, Kalia K, Borah A, Wang X, Dave KR, Rodriguez AM, Yavagal DR, Bhattacharya P (2019) Endoplasmic reticulum-mitochondria crosstalk: from junction to function across neurological disorders. Ann N Y Acad Sci 1457 (1):41-60. http://dx.doi.org/10.1111/nyas.14212
26. Guardia-Laguarta C, Area-Gomez E, Rub C, Liu Y, Magrane J, Becker D, Voos W, Schon EA, Przedborski S (2014) alpha-Synuclein is localized to mitochondria-associated ER membranes. J Neurosci 34 (1):249-259. http://dx.doi.org/10.1523/JNEUROSCI.2507-13.2014
27. Rane P, Sarmah D, Bhute S, Kaur H, Goswami A, Kalia K, Borah A, Dave KR, Sharma N, Bhattacharya P (2019) Novel Targets for Parkinson's Disease: Addressing Different Therapeutic Paradigms and Conundrums. ACS Chem Neurosci 10 (1):44-57. http://dx.doi.org/10.1021/acschemneuro.8b00180
28. Cali T, Ottolini D, Negro A, Brini M (2013) Enhanced parkin levels favor ER-mitochondria crosstalk and guarantee Ca(2+) transfer to sustain cell bioenergetics. Biochim Biophys Acta 1832 (4):495-508. http://dx.doi.org/10.1016/j.bbadis.2013.01.004
29. Zheng L, Bernard-Marissal N, Moullan N, D'Amico D, Auwerx J, Moore DJ, Knott G, Aebischer P, Schneider BL (2017) Parkin functionally interacts with PGC-1alpha to preserve mitochondria and

protect dopaminergic neurons. Hum Mol Genet 26 (3):582-598. http://dx.doi.org/10.1093/hmg/ddw418

30. Bajenaru ML, Zhu Y, Hedrick NM, Donahoe J, Parada LF, Gutmann DH (2002) Astrocyte-specific inactivation of the neurofibromatosis 1 gene (NF1) is insufficient for astrocytoma formation. Mol Cell Biol 22 (14):5100-5113. http://dx.doi.org/10.1128/MCB.22.14.5100-5113.2002
31. Zhang YH, Wang DW, Xu SF, Zhang S, Fan YG, Yang YY, Guo SQ, Wang S, Guo T, Wang ZY, Guo C (2018) alpha-Lipoic acid improves abnormal behavior by mitigation of oxidative stress, inflammation, ferroptosis, and tauopathy in P301S Tau transgenic mice. Redox Biol 14:535-548. http://dx.doi.org/10.1016/j.redox.2017.11.001
32. Guo C, Wang P, Zhong ML, Wang T, Huang XS, Li JY, Wang ZY (2013) Deferoxamine inhibits iron induced hippocampal tau phosphorylation in the Alzheimer transgenic mouse brain. Neurochem Int 62 (2):165-172. http://dx.doi.org/10.1016/j.neuint.2012.12.005
33. Guo C, Zhang YX, Wang T, Zhong ML, Yang ZH, Hao LJ, Chai R, Zhang S (2015) Intranasal deferoxamine attenuates synapse loss via up-regulating the P38/HIF-1alpha pathway on the brain of APP/PS1 transgenic mice. Front Aging Neurosci 7:104. http://dx.doi.org/10.3389/fnagi.2015.00104
34. Qian H, Kang X, Hu J, Zhang D, Liang Z, Meng F, Zhang X, Xue Y, Maimon R, Dowdy SF, Devaraj NK, Zhou Z, Mobley WC, Cleveland DW, Fu XD (2020) Reversing a model of Parkinson's disease with in situ converted nigral neurons. Nature 582 (7813):550-556. http://dx.doi.org/10.1038/s41586-020-2388-4
35. Genaro-Mattos TC, Anderson A, Allen LB, Korade Z, Mirnics K (2019) Cholesterol Biosynthesis and Uptake in Developing Neurons. ACS Chem Neurosci 10 (8):3671-3681. http://dx.doi.org/10.1021/acschemneuro.9b00248
36. Cheng X, Feng H, Wu H, Jin Z, Shen X, Kuang J, Huo Z, Chen X, Gao H, Ye F, Ji X, Jing X, Zhang Y, Zhang T, Qiu W, Zhao R (2018) Targeting autophagy enhances apatinib-induced apoptosis via endoplasmic reticulum stress for human colorectal cancer. Cancer Lett 431:105-114. http://dx.doi.org/10.1016/j.canlet.2018.05.046
37. Ding XW, Sun X, Shen XF, Lu Y, Wang JQ, Sun ZR, Miao CH, Chen JW (2019) Propofol attenuates TNF-alpha-induced MMP-9 expression in human cerebral microvascular endothelial cells by inhibiting Ca(2+)/CAMK II/ERK/NF-kappaB signaling pathway. Acta Pharmacol Sin 40 (10):1303-1313. http://dx.doi.org/10.1038/s41401-019-0258-0
38. Enzo E, Santinon G, Pocaterra A, Aragona M, Bresolin S, Forcato M, Grifoni D, Pession A, Zanconato F, Guzzo G, Bicciato S, Dupont S (2015) Aerobic glycolysis tunes YAP/TAZ transcriptional activity. EMBO J 34 (10):1349-1370. http://dx.doi.org/10.15252/embj.201490379
39. Song S, Tan J, Miao Y, Li M, Zhang Q (2017) Crosstalk of autophagy and apoptosis: Involvement of the dual role of autophagy under ER stress. J Cell Physiol 232 (11):2977-2984. http://dx.doi.org/10.1002/jcp.25785
40. Trist BG, Hare DJ, Double KL (2019) Oxidative stress in the aging substantia nigra and the etiology of Parkinson's disease. Aging Cell 18 (6):e13031. http://dx.doi.org/10.1111/acel.13031

41. Huang L, Chen R, Liu L, Zhou Y, Chen Z (2021) Lactoferrin ameliorates pathological cardiac hypertrophy related to mitochondrial quality control in aged mice. Food Funct 12 (16):7514-7526. http://dx.doi.org/10.1039/d0fo03346d
42. Subramaniam SR, Chesselet MF (2013) Mitochondrial dysfunction and oxidative stress in Parkinson's disease. Prog Neurobiol 106-107:17-32. http://dx.doi.org/10.1016/j.pneurobio.2013.04.004
43. Yan T, Zhao Y (2020) Acetaldehyde induces phosphorylation of dynamin-related protein 1 and mitochondrial dysfunction via elevating intracellular ROS and Ca(2+) levels. Redox Biol 28:101381. http://dx.doi.org/10.1016/j.redox.2019.101381
44. Cheng H, Gang X, He G, Liu Y, Wang Y, Zhao X, Wang G (2020) The Molecular Mechanisms Underlying Mitochondria-Associated Endoplasmic Reticulum Membrane-Induced Insulin Resistance. Front Endocrinol (Lausanne) 11:592129. http://dx.doi.org/10.3389/fendo.2020.592129
45. Chen Y, Zheng Z, Zhu X, Shi Y, Tian D, Zhao F, Liu N, Huppi PS, Troy FA, 2nd, Wang B (2015) Lactoferrin Promotes Early Neurodevelopment and Cognition in Postnatal Piglets by Upregulating the BDNF Signaling Pathway and Polysialylation. Mol Neurobiol 52 (1):256-269. http://dx.doi.org/10.1007/s12035-014-8856-9
46. Guo JJ, Yue F, Song DY, Bousset L, Liang X, Tang J, Yuan L, Li W, Melki R, Tang Y, Chan P, Guo C, Li JY (2021) Intranasal administration of alpha-synuclein preformed fibrils triggers microglial iron deposition in the substantia nigra of Macaca fascicularis. Cell Death Dis 12 (1):81. http://dx.doi.org/10.1038/s41419-020-03369-x
47. Maneva A, Taleva B, Maneva L (2003) Lactoferrin-protector against oxidative stress and regulator of glycolysis in human erythrocytes. Z Naturforsch C J Biosci 58 (3-4):256-262. http://dx.doi.org/10.1515/znc-2003-3-420
48. Rousseau E, Michel PP, Hirsch EC (2013) The iron-binding protein lactoferrin protects vulnerable dopamine neurons from degeneration by preserving mitochondrial calcium homeostasis. Mol Pharmacol 84 (6):888-898. http://dx.doi.org/10.1124/mol.113.087965
49. Welchen E, Gonzalez DH (2016) Cytochrome c, a hub linking energy, redox, stress and signaling pathways in mitochondria and other cell compartments. Physiol Plant 157 (3):310-321. http://dx.doi.org/10.1111/ppl.12449
50. Matsuyama S, Reed JC (2000) Mitochondria-dependent apoptosis and cellular pH regulation. Cell Death Differ 7 (12):1155-1165. http://dx.doi.org/10.1038/sj.cdd.4400779
51. Clark EH, Vazquez de la Torre A, Hoshikawa T, Briston T (2021) Targeting mitophagy in Parkinson's disease. J Biol Chem 296:100209. http://dx.doi.org/10.1074/jbc.REV120.014294
52. Xiao T, Liang X, Liu H, Zhang F, Meng W, Hu F (2020) Mitochondrial stress protein HSP60 regulates ER stress-induced hepatic lipogenesis. J Mol Endocrinol 64 (2):67-75. http://dx.doi.org/10.1530/JME-19-0207
53. Feng ST, Wang ZZ, Yuan YH, Wang XL, Sun HM, Chen NH, Zhang Y (2020) Dynamin-related protein 1: A protein critical for mitochondrial fission, mitophagy, and neuronal death in Parkinson's disease.

Pharmacol Res 151:104553. http://dx.doi.org/10.1016/j.phrs.2019.104553

54. Han XJ, Lu YF, Li SA, Kaitsuka T, Sato Y, Tomizawa K, Nairn AC, Takei K, Matsui H, Matsushita M (2008) CaM kinase I alpha-induced phosphorylation of Drp1 regulates mitochondrial morphology. J Cell Biol 182 (3):573-585. http://dx.doi.org/10.1083/jcb.200802164
55. Kennedy MB (2000) Signal-processing machines at the postsynaptic density. Science 290 (5492):750-754. http://dx.doi.org/10.1126/science.290.5492.750
56. Prasuhn J, Davis RL, Kumar KR (2020) Targeting Mitochondrial Impairment in Parkinson's Disease: Challenges and Opportunities. Front Cell Dev Biol 8:615461. http://dx.doi.org/10.3389/fcell.2020.615461
57. Surmeier DJ, Schumacker PT (2013) Calcium, bioenergetics, and neuronal vulnerability in Parkinson's disease. J Biol Chem 288 (15):10736-10741. http://dx.doi.org/10.1074/jbc.R112.410530
58. Cali T, Ottolini D, Negro A, Brini M (2012) alpha-Synuclein controls mitochondrial calcium homeostasis by enhancing endoplasmic reticulum-mitochondria interactions. J Biol Chem 287 (22):17914-17929. http://dx.doi.org/10.1074/jbc.M111.302794
59. Szymanski J, Janikiewicz J, Michalska B, Patalas-Krawczyk P, Perrone M, Ziolkowski W, Duszynski J, Pinton P, Dobrzyn A, Wieckowski MR (2017) Interaction of Mitochondria with the Endoplasmic Reticulum and Plasma Membrane in Calcium Homeostasis, Lipid Trafficking and Mitochondrial Structure. Int J Mol Sci 18 (7). http://dx.doi.org/10.3390/ijms18071576
60. Naon D, Zaninello M, Giacomello M, Varanita T, Grespi F, Lakshminaranayan S, Serafini A, Semenzato M, Herkenne S, Hernandez-Alvarez MI, Zorzano A, De Stefani D, Dorn GW, 2nd, Scorrano L (2016) Critical reappraisal confirms that Mitofusin 2 is an endoplasmic reticulum-mitochondria tether. Proc Natl Acad Sci U S A 113 (40):11249-11254. http://dx.doi.org/10.1073/pnas.1606786113
61. Aufschnaiter A, Kohler V, Diessl J, Peselj C, Carmona-Gutierrez D, Keller W, Buttner S (2017) Mitochondrial lipids in neurodegeneration. Cell Tissue Res 367 (1):125-140. http://dx.doi.org/10.1007/s00441-016-2463-1
62. Area-Gomez E, Schon EA (2016) Mitochondria-associated ER membranes and Alzheimer disease. Curr Opin Genet Dev 38:90-96. http://dx.doi.org/10.1016/j.gde.2016.04.006
63. Area-Gomez E, Del Carmen Lara Castillo M, Tambini MD, Guardia-Laguarta C, de Groof AJ, Madra M, Ikenouchi J, Umeda M, Bird TD, Sturley SL, Schon EA (2012) Upregulated function of mitochondria-associated ER membranes in Alzheimer disease. EMBO J 31 (21):4106-4123. http://dx.doi.org/10.1038/emboj.2012.202
64. Prasad M, Kaur J, Pawlak KJ, Bose M, Whittal RM, Bose HS (2015) Mitochondria-associated endoplasmic reticulum membrane (MAM) regulates steroidogenic activity via steroidogenic acute regulatory protein (StAR)-voltage-dependent anion channel 2 (VDAC2) interaction. J Biol Chem 290 (5):2604-2616. http://dx.doi.org/10.1074/jbc.M114.605808
65. Dagher R, Massie R, Gentil BJ (2021) MTP deficiency caused by HADHB mutations: Pathophysiology and clinical manifestations. Mol Genet Metab 133 (1):1-7. http://dx.doi.org/10.1016/j.ymgme.2021.03.010

66. Elustondo P, Martin LA, Karten B (2017) Mitochondrial cholesterol import. Biochim Biophys Acta Mol Cell Biol Lipids 1862 (1):90-101. http://dx.doi.org/10.1016/j.bbalip.2016.08.012
67. Jefcoate CR, Lee J (2018) Cholesterol signaling in single cells: lessons from STAR and sm-FISH. J Mol Endocrinol 60 (4):R213-R235. http://dx.doi.org/10.1530/JME-17-0281
68. Grunewald A, Kumar KR, Sue CM (2019) New insights into the complex role of mitochondria in Parkinson's disease. Prog Neurobiol 177:73-93. http://dx.doi.org/10.1016/j.pneurobio.2018.09.003

Tables

Table 1. List of biological reagents antibody

Antibody	Source	Manufacturer	Dilution ratio
α-synuclein	mouse	Thermo Fisher	1:1000
ATG5	mouse	Immunoway	1:1000
Bax	rabbit	Santa Cruz	1:1000
Bcl-2	mouse	Santa Cruz	1:1000
Calmodulin	mouse	Thermo Fisher	1:2000
Calreticulin	rabbit	Cell Signaling Tech	1:2000
p-CAMKIIα	rabbit	Abcam	1:2000
CAMKIIα	rabbit	Abcam	1:2000
caspase3	rabbit	Cell Signaling Tech	1:1000
COX4	rabbit	Thermo Fisher	1:3000
CytC	rabbit	Proteintech	1:1000
DAT	rat	Millipore	1:3000
DMT1	rabbit	Abcam	1:2000
p-Drp1	rabbit	Bioss	1:1000
Drp1	rabbit	Bioss	1:1000
p-EIF2α	rabbit	Immunoway	1:1000
EIF2α	rabbit	Immunoway	1:1000
Fpn	goat	Santa Cruz	1:1000
GPX4	rabbit	Cell Signaling Tech	1:1000
HSP60	mouse	Thermo Fisher	1:2000
Mfn2	rabbit	Bioss	1:1000
NMDAR2B	rabbit	Sigma-Aldrich	1:3000
PARK2/Parkin	mouse	Proteintech	1:1000
PINK1	rabbit	Proteintech	1:1000
SOD1	rabbit	Cell Signaling Tech	1:1000
TFR	mouse	Invitrogen	1:1000
TH	rabbit	Millipore	1:3000
xCT	rabbit	Abcam	1:1000

β-actin	mouse	Sigma-Aldrich	1:10000

Figures

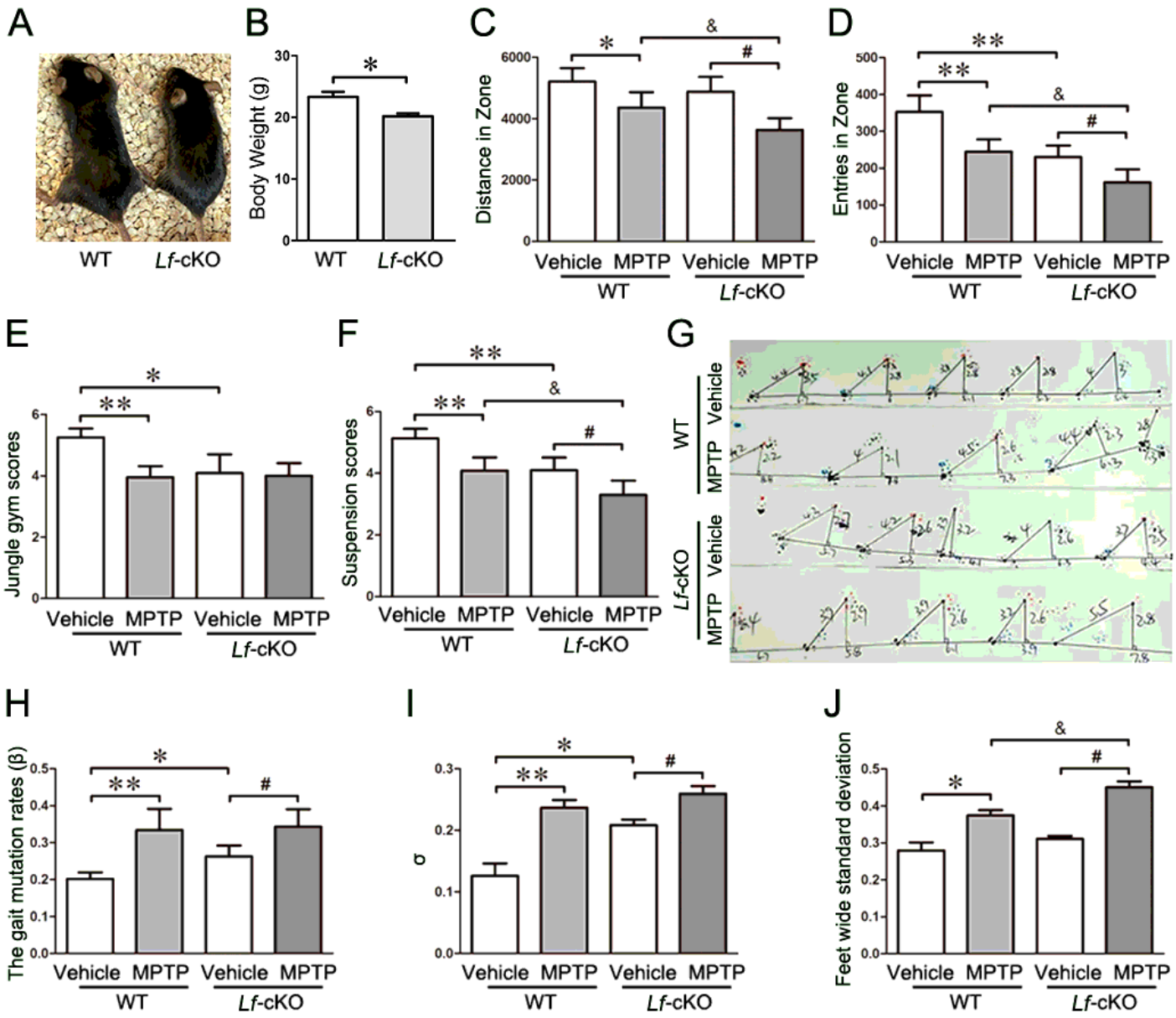

Figure 1

Astrocyte-specific loss of *Lf* increases MPTP-induced behavioral and emotional disorder

(A) The body size of 3-month-old *Lf*-cKO mice were compared with that of control mice. (B) The weight statistics of WT and *Lf*-cKO mice were counted in 90 days. (C) Total distance traveled during 5 min of open field exploration. (D) Entries in zone-center showing 5 min of open field exploration by the mice. (E) Jungle gym score of pole-climbing test. (F) Suspension scores of traction test. (G) Gait analysis diagram

of gait analysis experiment. (H) The gait mutation rates (β) of gait analysis experiment. (I) Average variance of the distance between two adjacent left footprints (σ) of gait analysis experiment. (J) Feet wide standard deviation of gait analysis experiment. Values correspond to the mean ± SEM. *$p < 0.05$, **$p < 0.01$ compared with the WT control group; #$p < 0.05$ compared with the *Lf*-cKO control group; &$p < 0.05$ compared with the WT MPTP group.

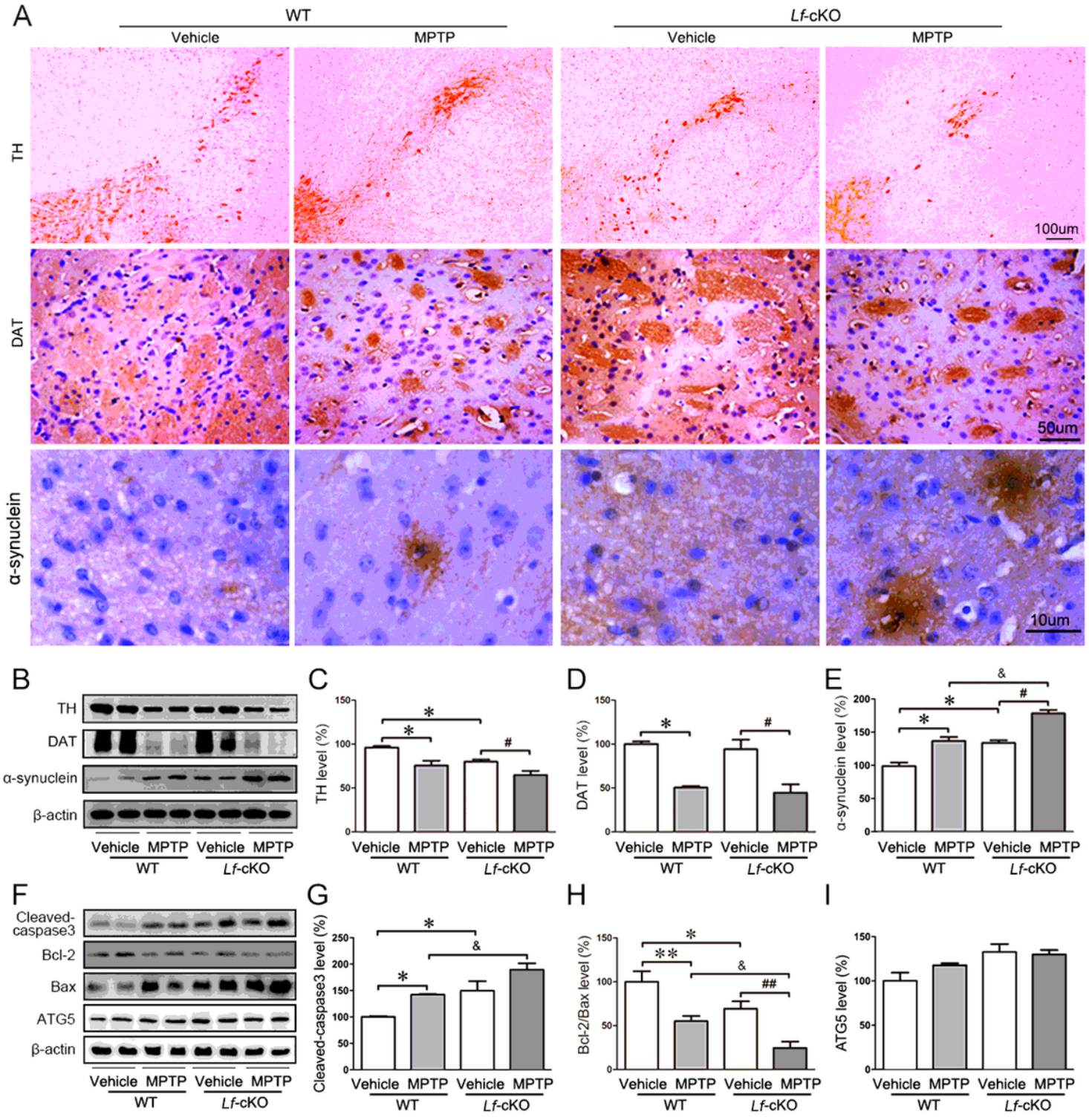

Figure 2

DA neuron degeneration is more pronounced in MPTP-treated Lf-cKO mice

(A) The levels of TH, DAT and α-synuclein were measured by immunostaining analysis (n = 5). Scale bars = 100 μm, 50 μm, 10μm. (B-E) The expressions of TH, DAT and α-synuclein were determined by western blot analyses (n = 8). (F-I) Western blot results showed the protein expression levels of cleaved-caspase3, Bcl-2, Bax and ATG5 of four groups of mice and the quantitative analysis chart (n = 8). Values are represented as the means ± SEM. *$p < 0.05$, **$p < 0.01$ compared with the WT control group; #$p < 0.05$, ##$p < 0.01$ compared with the *Lf*-cKO control group; &$p < 0.05$ compared with the WT MPTP group.

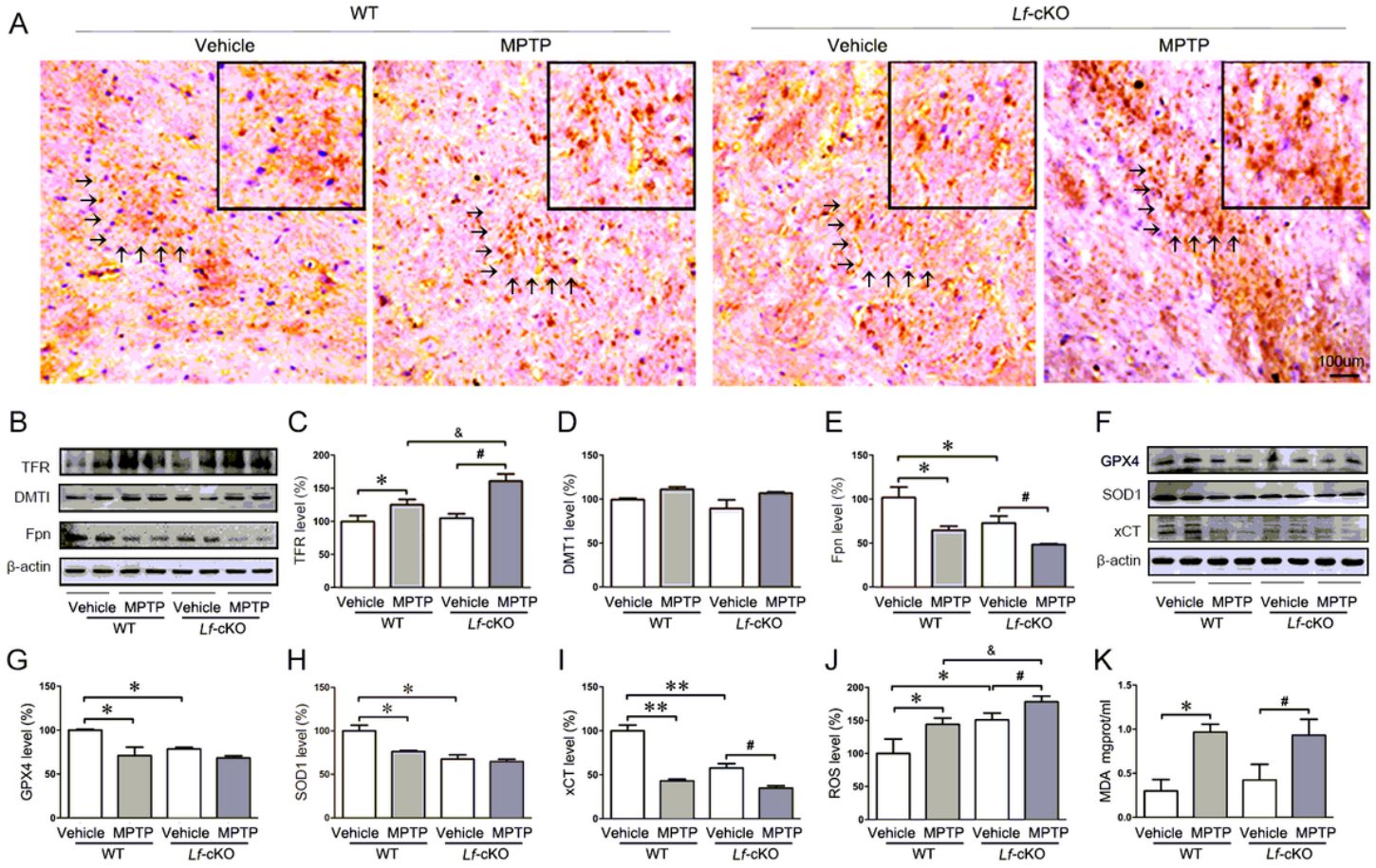

Figure 3

Astrocytic Lf deficiency induces iron metabolism disorder and aggravates oxidative stress in MPTP-treated mice

(A) Modified Prussian DAB staining showed a clear change in the iron distribution among four treatments and the quantitative analysis of DAB staining in SN (n = 5). Scale bar = 100 μm. (B-E) Western blot results showed the protein expression levels of TFR, DMT1 and Fpn of four groups of mice and the quantitative analysis chart (n = 8). (F) Changes in expression levels of GPX4, SOD1 and xCT in mice brains SN by western blots. Quantitative analysis of the proteins shown in G-I (n = 8). (J) ROS content was detected by test kit (n = 5). (K) The content of MDA was detected by test kit (n = 5). Values are represented as the

mean ± SEM. *$p < 0.05$, **$p < 0.01$ compared with the WT control group; #$p < 0.05$ compared with the *Lf*-cKO control group; &$p < 0.05$ compared with the WT MPTP group.

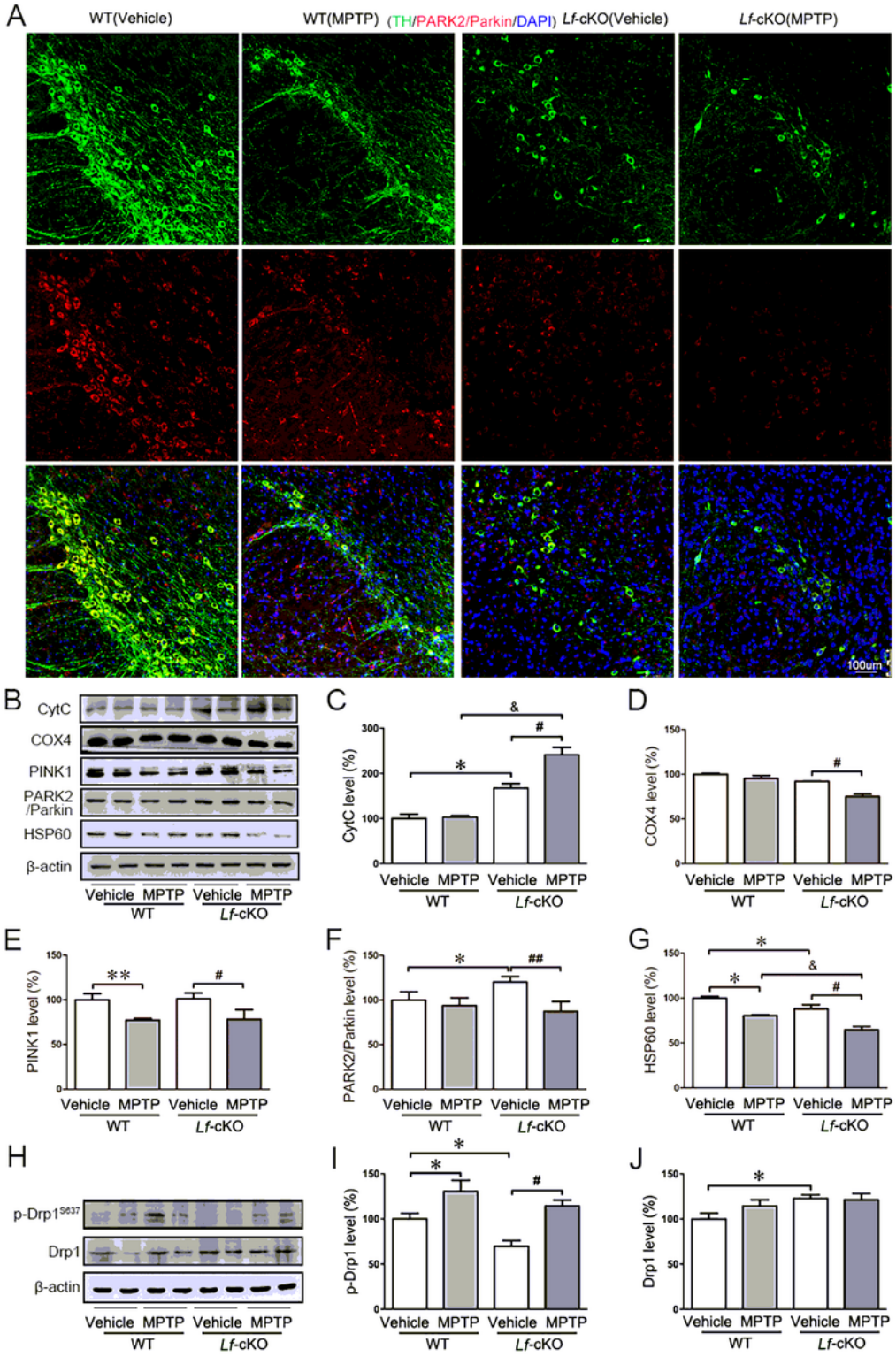

Figure 4

Astrocytic Lf deficiency leads to mitochondrial dysfunction of dopaminergic neurons and is aggravated after MPTP treatment

(A) Immunofluorescence with TH and PARK2/Parkin in the SN. Scale bars = 100 μm (n = 3). (B-G) Western blot analysis of CytC, COX4, PINK1, PARK2/Parkin and HSP60 in the SN (n = 8). (H-J) Western blot was used to detect the expression of p-Drp1^{S637} and Drp1 in the SN (n = 8). The data were expressed in the form of mean ± SEM. *p < 0.05, **p < 0.01 compared with the WT control group; #p < 0.05, ##p < 0.01 compared with the *Lf*-cKO control group; &p < 0.05 compared with the WT MPTP group.

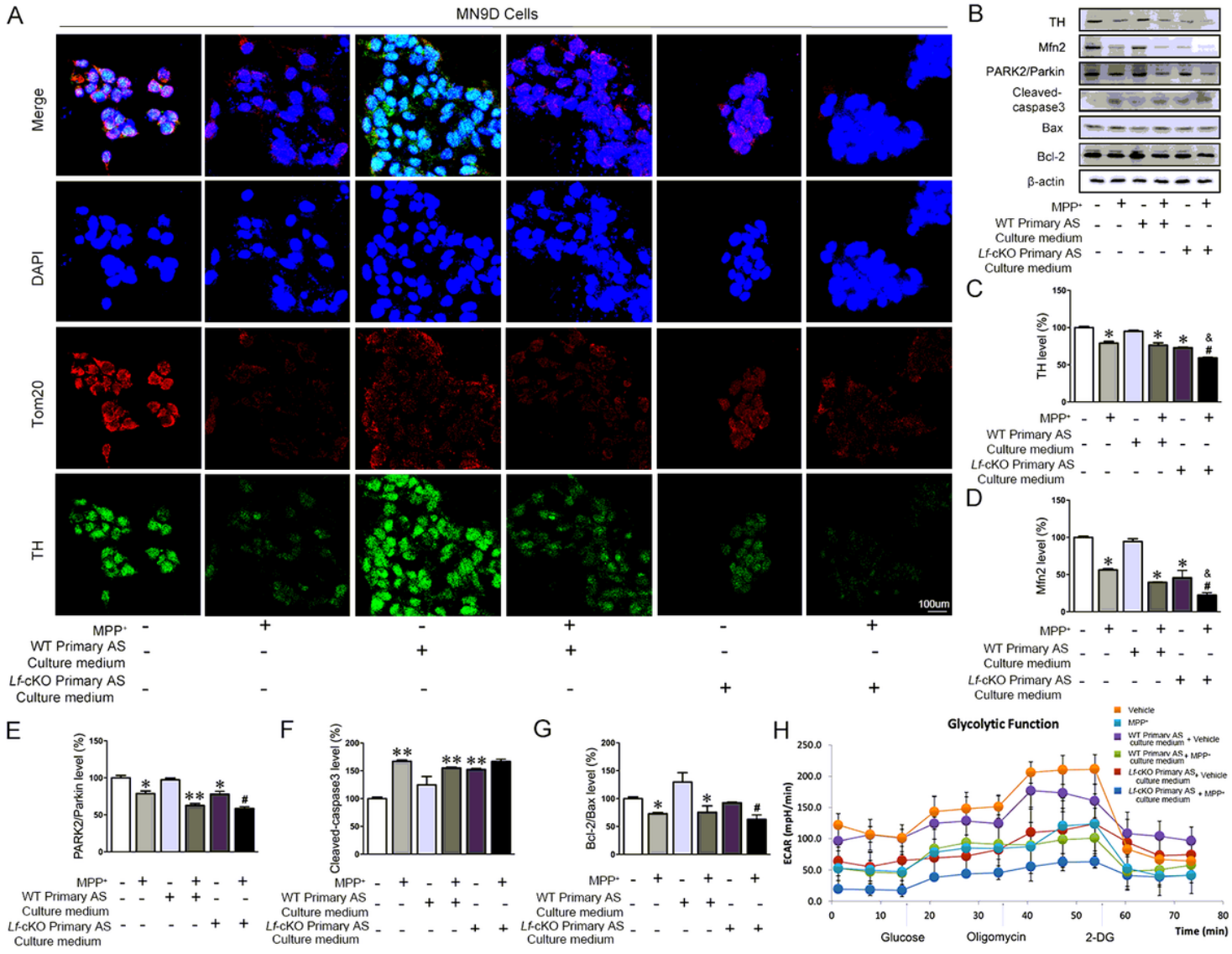

Figure 5

Astrocytic Lf deficiency induces mitochondrial dysfunction and neuronal apoptosis in vitro

(A) MN9D cells treated differently were observed by fluorescence microscopy after the cells were stained with Tom20 and TH following DAPI. Scale bar = 100 μm. (B-G) The expression levels of TH, Mfn2, PARK2/Parkin, cleaved-caspase3, Bax and Bcl-2 in MN9D cells treated differently were tested by immunoblotting and quantitative analyses of these proteins. (H) Representative ECAR profiles of MN9D cells treated differently. *p < 0.05, **p < 0.01 compared with the control group; #p < 0.05 compared with the *Lf*-cKO control group; &p < 0.05 compared with the MPP$^+$ group.

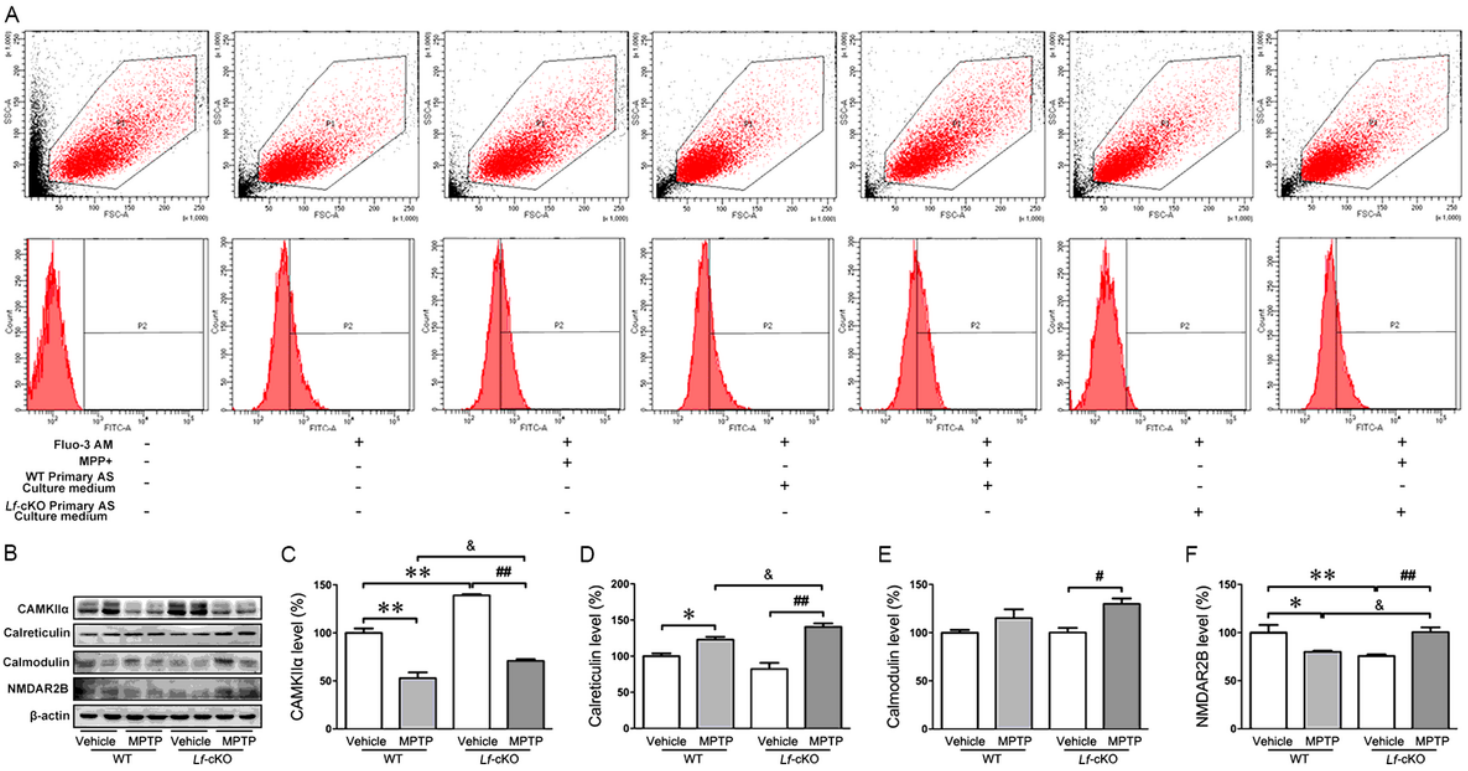

Figure 6

Astrocyte-derived Lf regulates calcium homeostasis in dopaminergic neurons

(A) Calcium concentrations in MN9D cells following different treatments were measured by flow cytometry. (B) Changes in the expression levels of CAMKIIα, calreticulin, calmodulin and NMDAR2B in the mouse brain SN were measured by Western blots. Quantitative analysis of the proteins shown in C-F (n = 8). The data were expressed in the form of mean ± SEM. *$p < 0.05$, **$p < 0.01$ compared with the WT control group; #$p < 0.05$, ##$p < 0.01$ compared with the *Lf*-cKO control group; &$p < 0.05$ compared with the WT MPTP group.

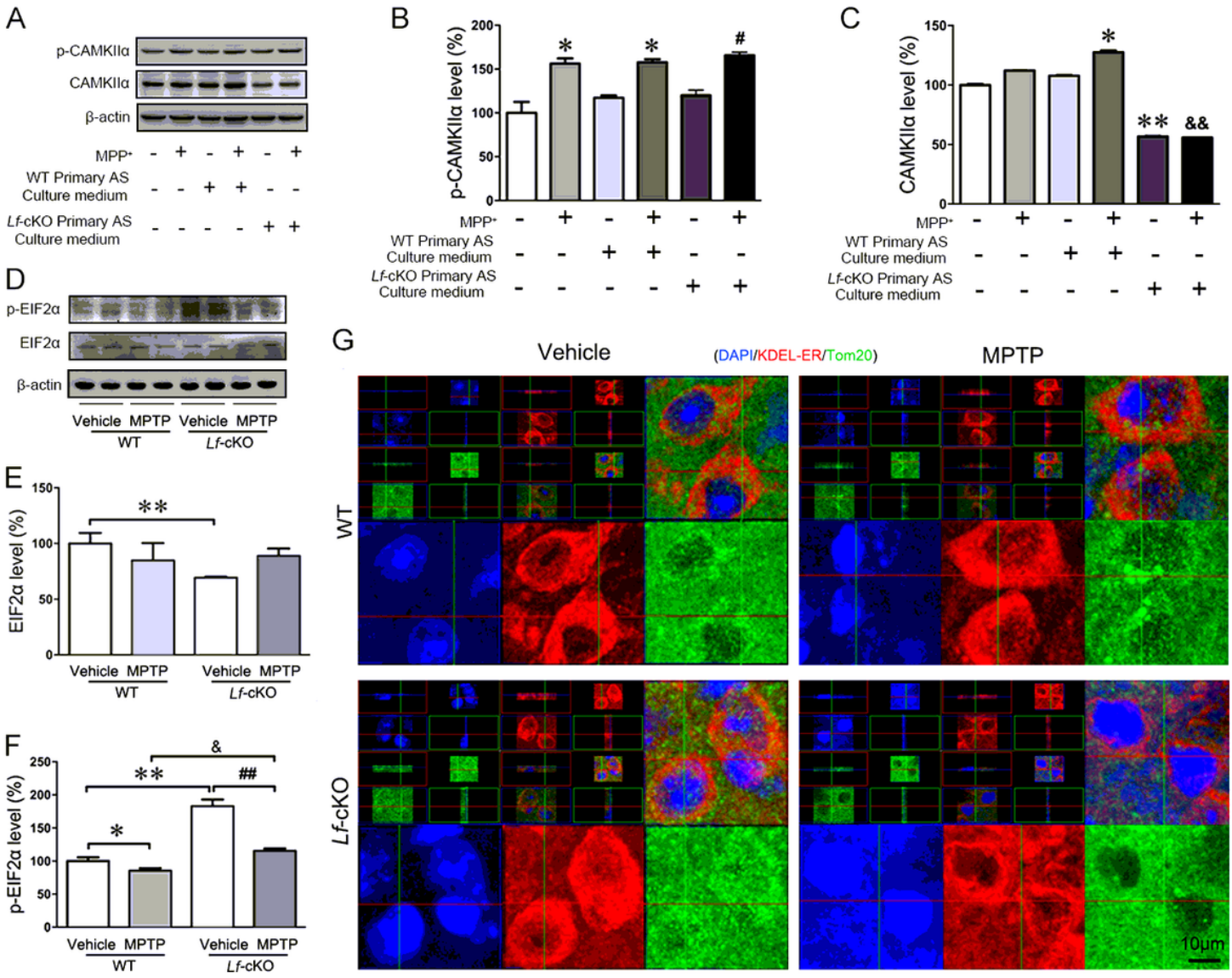

Figure 7

Astrocyte-derived Lf deficiency-induced intracellular calcium dyshomeostasis involves the ER

(A-C) Western blot was used to detect the expression of p-CAMKIIα and CAMKIIα in MN9D cells treated differently and quantitative analyses of these proteins. (D) The levels of p-EIF2α and EIF2α were detected by western blot in mice (n = 8), quantitative analysis of the proteins shown in E, F. (G) Fluorescence co-localization of mitochondria (Tom20, green) and ER (KDEL-ER, red) of dopamine neuron by fluorescence labelling in SN (n = 5). Scale bar = 10 μm. The data were expressed in the form of mean ± SEM. *$p < 0.05$, **$p < 0.01$ compared with the WT control group; #$p < 0.05$, ##$p < 0.01$ compared with the *Lf*-cKO control group; &$p < 0.05$ compared with the WT MPTP or MPP^+ group.

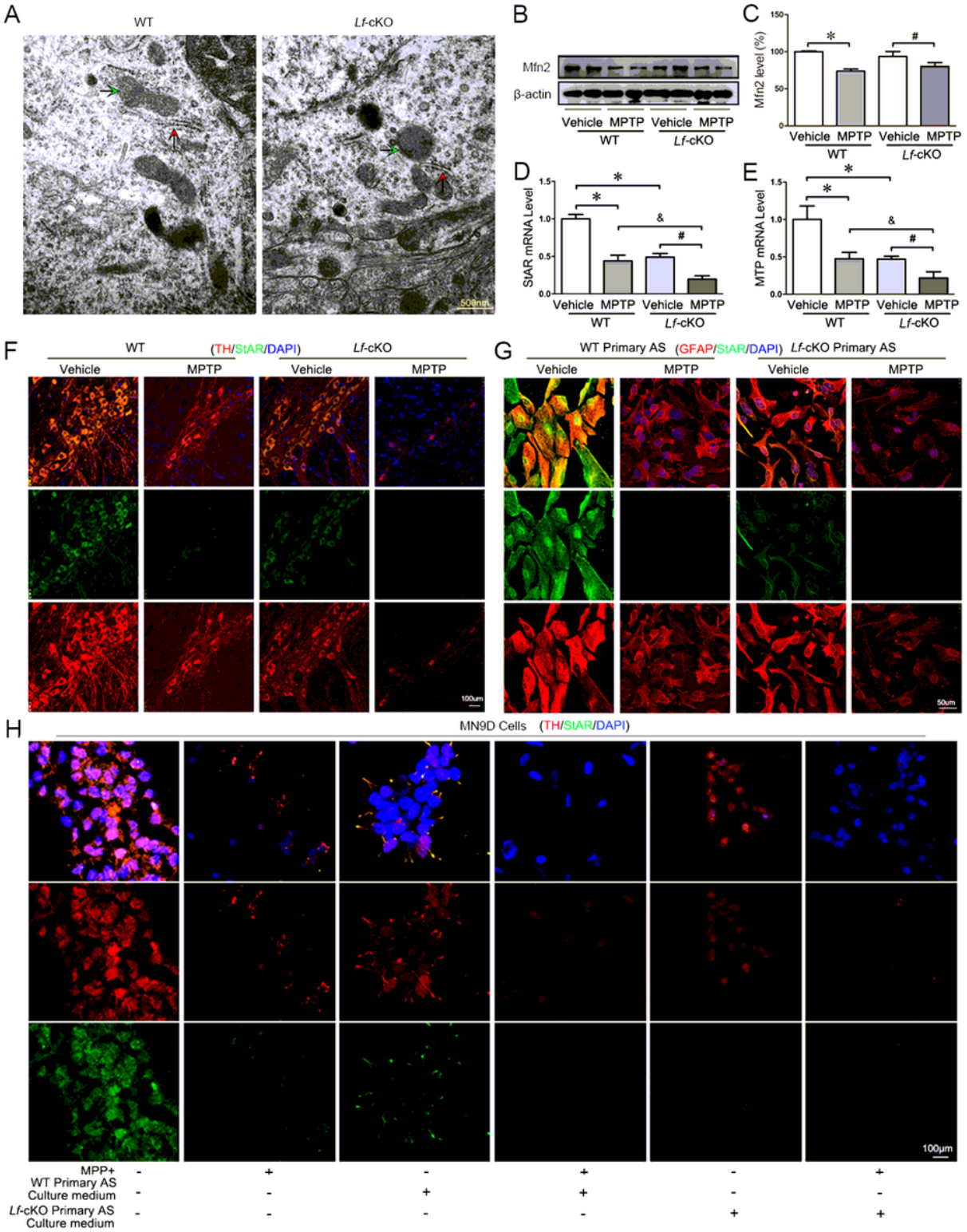

Figure 8

Astrocyte-derived Lf deficiency prevents mitochondrial lipid transport by affecting MAMs

(A) The contact sites of mitochondria and endoplasmic reticulum of WT and *Lf*-cKO mice was observed by electron microscopy, scale bar = 500 nm. (B, C) Western blot was used to detect the expression of Mfn2 in four group mice and its quantitative analysis (n = 8). (D) Quantitative Real-time PCR

measurements to determine StAR expression levels in mice (n = 5). (E) Quantitative Real-time PCR measurements to determine MTP expression levels in mice (n = 5). (F) Immunofluorescence was used to detect the expression of TH and StAR in SN of mice brain (n = 5), scale bar = 100 μm. (G) Immunofluorescence was used to detect the expression of GFAP and StAR in the primary astrocytes from WT and *Lf*-cKO newborn mice treated or untreated with MPP^+, scale bar = 50 μm. (H) Immunofluorescence was used to detect the expression of TH and StAR in MN9D cells treated differently, scale bar = 100 μm. The data were expressed in the form of mean ± SEM. *$p < 0.05$ compared with the WT control group; #$p < 0.05$ compared with the *Lf*-cKO control group; &$p < 0.05$ compared with the WT MPTP group.

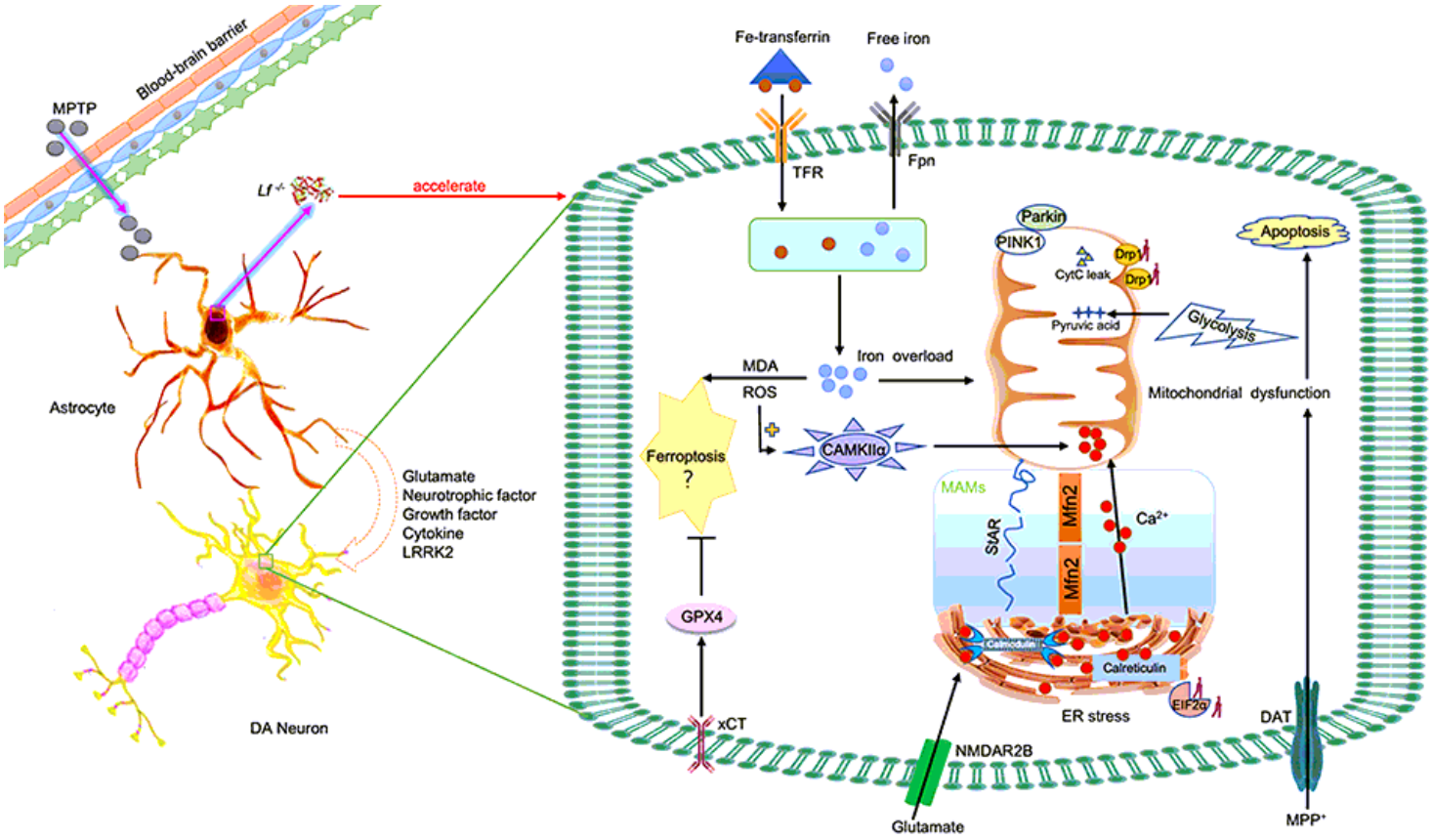

Figure 9

Schematic diagram of specific knockout of astrocyte *lactoferrin* accelerating the loss of dopamine neurons in the PD model.

MPTP is metabolized into MPP^+ in astrocytes and transferred into DA neurons through DAT, resulting in mitochondrial dysfunction and DA neuron apoptosis. Specific knockout of astrocyte *lactoferrin* changed the morphology and function, and the imbalance of calcium homeostasis led to mitochondrial dysfunction and apoptosis. Astrocytic calcium imbalance triggers astrocytes to release glutamate and other cytokines. This information is fed back to DA neurons, causing the increase of Ca^{2+} concentration

by NMDAR2B, which induces a large amount of Ca^{2+} in the ER to flow into mitochondria, affects mitochondrial related lipid metabolism and accelerates cells apoptosis.

Supplementary Files

This is a list of supplementary files associated with this preprint. Click to download.

- SupplementaryInformation.pdf
- floatimage1.jpeg